QRS Complex Detection in Experimental Orthogonal Electrograms of Isolated Rabbit Hearts

Jiri Kozumplik[1], Marina Ronzhina[1,2], Oto Janousek[1,2], Jana Kolarova[1,2], Marie Novakova[2,3], Ivo Provaznik[1,2]

[1]Department of Biomedical Engineering, Brno University of Technology, Brno, Czech Republic
[2]International Clinical Research Center, St. Anne's University Hospital Brno, Brno, Czech Republic
[3]Department of Physiology, Faculty of Medicine, Masaryk University, Brno, Czech Republic

Abstract

Automated analysis of HRV and/or QT intervals of isolated rabbit heart electrograms requires reliable detection of QRS complexes. We propose a detection method based on spatial velocity using differentiation of all lead signals, the squaring, the adding and the square root in orders. Teager-Kaiser energy operator was applied after filtering spatial velocity with a standard pass-band filter. The algorithm was tested on 263 orthogonal electrograms. Resulting values of both sensitivity and positive predictive value of detection increased 99.8%.

1. Introduction

Detection of QRS complexes in ECG signals is required for the automatic analysis of these signals. There are many different algorithms for the detection of the QRS complexes in human ECG signals. Brief descriptions of the principles of many of them including comparison of their properties and efficiency can be found for example in [1]. A number of other algorithms were published till recently. One of the most reliable algorithms is based on wavelet transform [2]. Modifications of the method of Pan and Tompkins [3] are highly cited and often used, most probably for their simple applicability.

Analysis of electrograms recorded from isolated animal hearts is carried out only on a few sites and publications aimed at the detection of QRS complexes in these signals are not available.

A number of algorithms designed for human signals could be used for the detection of QRS complexes in animal electrograms either directly or after minor modifications. Both types of signals, however, often differ in the spectra of their individual parts. The most striking difference is in the spectra of P waves, which significantly overlap with the spectra of subsequent QRS complexes in some leads. In such leads, the detector can produce false positive detection of the QRS complex (or R wave) in the area of P waves.

QRS complex detectors used for processing human signals are generally implemented as single lead detectors [1], [2]. In case of multiple lead signals, the detector can then be used lead-by-lead and individual results of each detection can be combined to exclude false-positive or false negative detection. False detections are expected in less than half of the leads.

Electrograms processed in the project were recorded from three orthogonal leads. We used a detector based on spatial velocity signal calculated from the first difference of the signals from orthogonal leads. After filtering this signal with a suitable bandpass filter, we used Teager-Kaiser energy operator [4], [5] followed by thresholding.

2. Methods

2.1. ECG recording

The experiments were performed in accordance with the guidelines for animal treatment approved by local authorities and conformed to the EU law. Experimental electrograms (EGs) were recorded from isolated New Zealand rabbit hearts during global ischemia study. Heart function was stabilized for 15–20 minutes followed by application of fluorescent dye di-4-ANEPPS for optical recording. In the experimental part, the heart was subjected to 15 minutes of global ischemia followed by 15 minutes of reperfusion repeated in three cycles. Global ischemia was induced by stopping flow of the solution into the heart.

Measurement was performed by touch-less method using three pairs of Ag-AgCl electrodes placed in an orthogonal coordinates X, Y, Z on an interior wall of buffer-filled glass chamber. All data was acquired by USB-6259 acquisition card (National Instruments) in 16-bit resolution and sampling frequency f_s = 2000 Hz.

Some intervals of the signal were affected by power supply interference (50 Hz) and by isoline step changes caused by manipulation with electrode system.

More details about our rabbit heart EG database were reported in [4], database is freely available in http://www.ubmi.feec.vutbr.cz/cardio/www/.

QRS detection algorithms were tested on a database containing 263 three-lead signals of 10 second length. The database was created for the purpose of testing methods for the analysis of those signals.

2.2. QRS complex detection

Electrograms were recorded from orthogonal leads *x*, *y*, *z*. Detection process is presented in Fig.1. First, the spatial velocity signal *v* was calculated from all lead signals by using first differences,

$$v(n) = \sqrt{\begin{matrix}[x(n) - x(n-1)]^2 + [y(n) - y(n-1)]^2 \\ +[z(n) - z(n-1)]^2\end{matrix}} \quad (1)$$

The signal of spatial velocity was subsequently filtered by a bandpass filter whose cut-off frequencies were set at 15 and 25 Hz. The result is a signal v_{BP}. Cut-off frequency bandpass filter were adjusted based on experiments and their selection was influenced by signal v_{TKEO}. This signal resulted from application of nonlinear Teager-Kaiser energy operator (TKEO) [2] whose difference equation is (in non-casual form)

$$v_{TKEO}(n) = v_{BP}^2(n) - v_{BP}(n-1)v_{BP}(n+1) \quad (2)$$

TKEO calculation is based on the fact [4] that for the harmonic signal $x(n)$ with the frequency f and the varying amplitude $A(n)$ it is true at a sampling frequency f_s that

$$A^2(n)sin^2\omega_r = x(n) - x(n-1)x(n+1) \quad (3)$$

where

$$\omega_r = 2\pi\frac{f}{f_s} \quad (4)$$

when it is approximately true that

$$A^2(n)sin^2\omega_r \approx A^2\ \omega_r^2 \quad (5)$$

for

$$\omega_r < \frac{\omega_s}{4}\,. \quad (6)$$

Block diagram of the detector is shown on Fig.1.

TKEO therefore represents an estimate of instant energy of a harmonic signal. For a narrowband signal, as in our case, where the spatial velocity signal is filtered with narrow band-pass filter, a similar result can be expected.

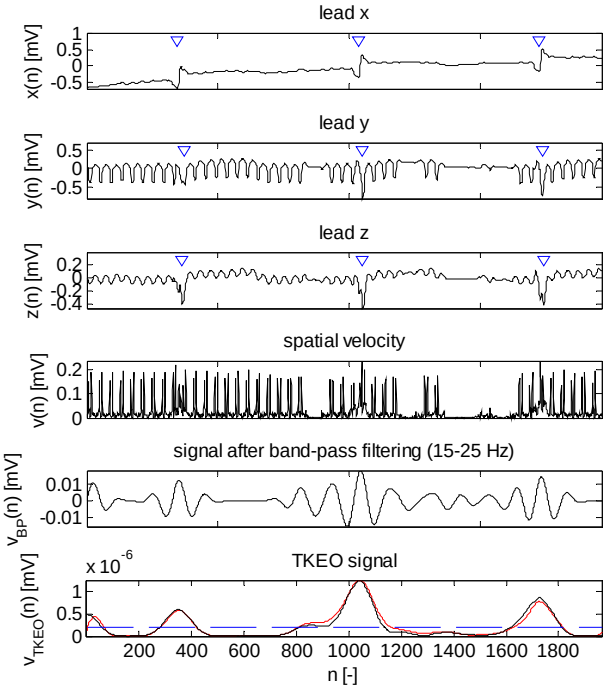

Figure 2. Part of three-lead EG (lead *x*, lead *y*, lead *z*), space velocity, the signal after filtering space velocity and the resulting signal TKEO (black) and quadrate envelopes (red) with a threshold (blue).

Thresholding is the last step of the detection, where the threshold is set at 15% of maximum of TKEO signal in the analysed interval. Figure 2 shows an example of outputs of the blocks depicted in Figure 1. The procedure resembles the method of Pan and Tompkins [2] applied to spatial velocity signal. The block with TKEO calculation is used instead of square envelope of the filtered signal. Its approximation can be obtained by low-pass filtering. Another option is to calculate the square of the envelope of the filtered signal. However, it is computationally

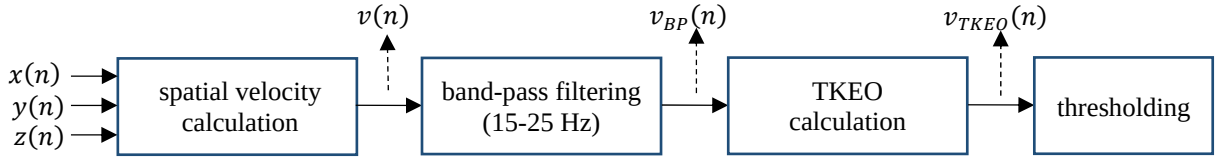

Figure 1. Block diagram of the QRS complex detector.

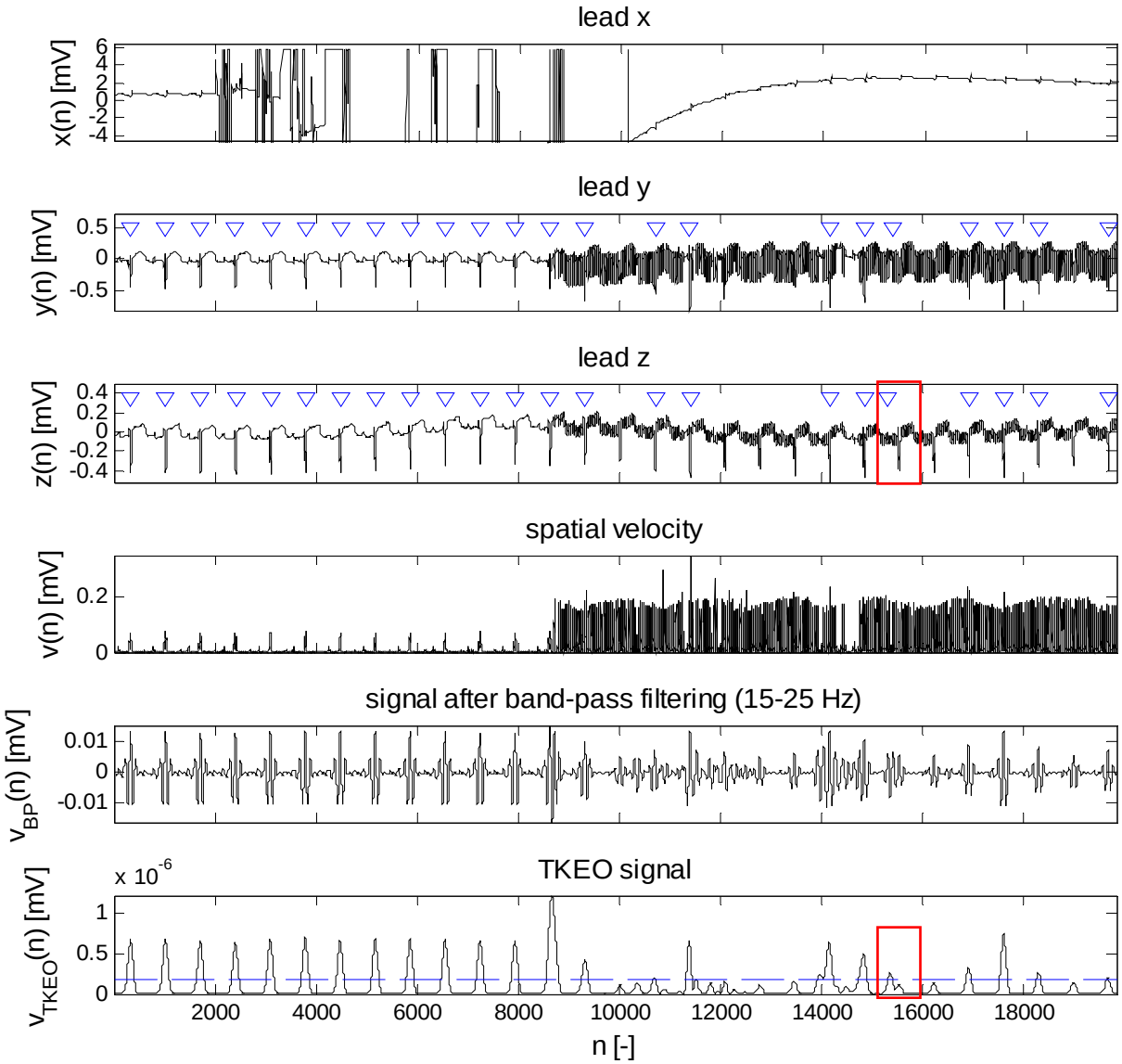

Figure 3. Automatic removal of incorrect lead *x*, QRS complex detection from leads *y* and *z* (signal No. 021).

demanding because an analytical signal must be first obtained. Its absolute value represents precisely the envelope signal [7]. Recall that the analytical signal is obtained using DFT of the input signal, zeroing half of its spectrum and IDFT. Alternatively, an analytical filter with a relatively long impulse response can be used in time domain. In our case, the narrowband signal is squared envelope signal very similar to the TKEO waveform, as it can be seen in Figure 2. Computational complexity of TKEO calculation is significantly lower than the precise envelope calculation.

The occurrence of the QRS complexes is expected in the interval where the signal TKEO exceeds the threshold. Extremes in QRS complexes are searched in individual leads within an interval around extreme of the TKEO signal, which is a 50 msec, 25 msec on either side of the extreme.

In some cases, especially for signals with a higher content of noise, there can be more than one main peak of the TKEO signal in the area of expected QRS complexes. In the case of neighbouring peaks above threshold with distance of extremes lower than 150 ms, we further considered only a higher extreme. Figure 3 shows false positive detection (marked by red box) caused by the influence of an extremely large disturbance.

The algorithm excludes leads in which the signal reaches values corresponding to the range of the used A/D converter, or there are high values of the first difference, which cannot occur in QRS complexes. Figure 3 shows that a signal from lead *x* was excluded from detection of because it is clearly inapplicable. Thus, only two leads were involved in the detection in this case.

However, the lead *y* contains significant interference which leads to seven false negative (FN) detections and to one false positive (FP) detection. In this case, the detection algorithm would only perfectly work on the single signal from *z* lead.

3. Results

The used processed signals from a database had a length of 10 seconds (20,000 samples for sampling frequency of 2 kHz). The signals were used in full length with the only setting of thresholds during testing the algorithm. The signals in the test database were relatively noise free with few exceptions. For signals No. 021 and 039, the algorithm excluded one lead with a totally corrupted signal. The signal No. 169 contained random sequences of narrow pulse interference in all leads. The block assessing the occurrence of the first differential signal excluded it from further analysis. Interfering pulses were suppressed with the use of median filter with a window length of $N = 5$. It appeared that the use of the median filter with such a short window does not lead to failure of detection of any of the other signals. The detector failed only in the case of signal No. 021, as shown in Figure 3.

The tested set of 263 signals contained 4492 cycles in total. The tests resulted in $FN = 7$ false negative detections and $FP = 1$ false positive detection. Thus, the sensitivity (probability of positive detection of the QRS complex) was $S = 99.84\%$ and positive predictive value (probability that the detected point truly represent a QRS complex) was $P = 99.98\%$.

4. Conclusions

The developed detector based on the spatial velocity and subsequent relatively simple digital signal processing was proved as reliable. Large P-waves whose power spectra coincided with the spectra of QRS complexes were found in 10 out of 789 leads. QRS complex detection in each of these 10 leads was difficult. However, resulting sensitivity and predictability is comparable to published QRS complex detector designed for analysis of human ECG signals. It was shown that processing of the signal with the use of Teager-Kaiser energy operator was significantly easier comparing to standard the envelope calculation.

Acknowledgements

Supported by grant project No. GACR 102/12/2034 and by European Regional Development Fund - Project FNUSA-ICRC (No. CZ.1.05/1.1.00/02.0123).

References

[1] Kohler B-U, Hennig C, Orglmeister R. The principles of software QRS detection. IEEE Engineering in Medicine and Biology Magazine 2002;21:42-57.

[2] Martínez JP, Almeida R, Olmos S, Rocha AP, Laguna P. A Wavelet-Based ECG Delineator: Evaluation on Standard Databases. IEEE Transactions on Biomedical Engineering 2004;51:570-581.

[3] Pan J, Tompkins WJ. A real-time QRS detection algorithm. IEEE Transactions on Biomedical Engineering 1985;32: 230-236.

[4] Kaiser JF. On a simple algorithm to calculate the 'energy' of a signal. IEEE International Conference Acoustic Speech Signal Process 1990:381-384.

[5] Solnik S, DeVita P, Rider P, Long B, Hortobagyi T. Teager-Kaiser operator improves the accuracy of EMG onset detection independent of signal-to-noise ratio 2008, Acta of Bioengineering and Biomechanics;10:65-68.

[6] Kolarova J, Novakova M, Ronzhina M, Janousek O, Vesely P, Olejnickova V, Provaznik I. The Isolated Rabbit Hearts - Databases of EGs and MAP Signals. Computing in Cardiology 2013;40:551-554.

[7] Jan J. Digital signal filtering, analysis and restoration. London: IEE, 2000.

Address for correspondence:

Ivo Provaznik
Department of Biomedical Engineering
Faculty of Electrical Engineering and Communication
Technicka 12
61200 Brno
Czech Republic
provaznik@feec.vutbr.cz.